Optik 151 (2017) 55–64

Contents lists available at ScienceDirect

Optik

journal homepage: www.elsevier.de/ijleo

SVM-based detection in visible light communications

Youli Yuan [a], Min Zhang [a,*], Pengfei Luo [b], Zabih Ghassemlooy [c], Lei Lang [d], Danshi Wang [a], Bo Zhang [a], Dahai Han [a]

[a] State Key Laboratory of Information Photonics and Optical Communications, Beijing University of Posts and Telecommunications, Beijing, 100876, China
[b] Research Department of HiSilicon, Huawei Technologies Co., Ltd, Beijing, 100085, China
[c] Optical Communications Research Group, NCRLab, Faculty of Engineering and Environment, Northumbria University, Newcastle upon Tyne, NE1 8ST, United Kingdom
[d] Science and Tech. on Info. Transmission and Dissemination in Comm. Networks Lab, Shijiazhuang, 050081, China

ARTICLE INFO

Article history:
Received 13 March 2017
Received in revised form 31 July 2017
Accepted 14 August 2017

Keywords:
Support vector machine
Superposed pulse amplitude modulation
Orthogonal frequency division multiplexing
Visible light communication
Direct decision

ABSTRACT

A support vector machine (SVM)-based data detection for 8-superposed pulse amplitude modulation and direct-current-biased optical orthogonal frequency division multiplexing in visible light communication is proposed and experimentally demonstrated. In this work, the SVM detector contains multiple binary classifiers with different classification strategies. The separating hyperplane of each SVM is constructed by means of the training data. The experiment results presented that the SVM detection offers improved bit error rate performance compared with the traditional direct decision method.

1. Introduction

With the increasing popularity of smart mobile devices, the wireless data traffic is growing exponentially [1]. This has resulted in shortage of the radio frequency (RF) spectrum and made the RF spectrum to become a precious and costly commodity. With the RF spectrum becoming congested there is the growing need to look for solutions that can alleviate the problem. Possible potions in the RF domains are frequency hopping and sharing, reduced interference, spectrum borrowing, new spectrum, more efficient spectrally efficient modulation schemes, reduced interference, etc. However, there is an alternative option of adopting the license free optical bands of infrared, ultraviolet and visible, which are categorized under the optical wireless communications (OWC) [2]. OWC offering an optical fiber type high transmission capacity is a complementary technology to the RF communications, which can be used in a number of indoor and outdoor applications in place of RF. Thus allowing the RF spectrum to be used in areas most particularly outdoor where mobility is paramount. In addition, the OWC technology could be used in applications such as hospitals, aircraft, mines etc., where RF-based electromagnetic interference is not allowed [3]. As a new lighting technology, we are seeing rapid installation of white light-emitting diodes (LEDs) at a global level, which helps to reduce the carbon footprint due to lighting. Consequently, this has created a golden opportunity to explore the multiple functionality of LEDs including data communications, indoor localization, and sensing. LEDs used for illuminations as well as data communications is known as the visible light communications (VLC) (or LiFi, which is the commercial name) technology, which could be used in both indoor and outdoor environments.

* Corresponding author. Tel.: +86 15101506278.
E-mail address: mzhang@bupt.edu.cn (M. Zhang).

https://doi.org/10.1016/j.ijleo.2017.08.089
0030-4026/

In VLC systems, the information signal is used to intensity modulate (IM) LEDs. On-off-keying (OOK) is one of the most widely used modulation formats, which is relatively easily to implement in hardware [4]. However, with OOK VLC the transmission data rate R_d is limited because of the low bandwidth of white LEDs (most commonly used), which is only several MHz due to the slow time constant of the yellow phosphor [5]. Hence, R_d of conventional OOK could only reach up to several Mbps. Consequently, several studies have been performed to increase R_d in VLC systems. First, quadrature amplitude modulation (QAM) with orthogonal frequency division multiplexing (OFDM) including direct-current-biased optical OFDM (DCO-OFDM) and asymmetrically clipped optical OFDM (ACO-OFDM) were widely used in VLC systems [6,7]. On the other hand, to avoid complexity of both transmitter (Tx) and the receiver (Rx), spatial modulation techniques were proposed with higher spectral efficiency as in [8–11]. Superposed pulse amplitude modulation (SPAM), which is low-cost, and insensitive to the non-linearity of LEDs, was proposed to reduce the complexity of the transceiver and enhance the frequency efficiency by $\log N$ times[11]. In SPAM, an N parallel NRZ-OOK signals with different amplitudes are used for IM of N-LEDs, whose optical power is then superposed in a free space channel to produce a 2^N-level signal. Following this principle, the Tx can provide a larger dynamic range than the traditional LED based system.

Machine learning has been widely employed to solve problems in different areas such as big data processing, personalized recommendation, pattern recognition, data mining and artificial intelligence, etc. [12]. What's more, this technique is used in VLC systems to reduce the effect of fluorescent light interference, inter-symbol interference (ISI) and artificial light interference [13–15]. In VLC systems, the background noise, electrical noise from transceiver and bandwidth limitation of LED contribute to the distortion of the received waveform. Amplitude modulation schemes such as pulse amplitude modulation (PAM) are especially sensitive to the signal distortion, which leads to poor performance in IM/direct detection (DD) based VLC systems.

Support vector machine (SVM) is one of the powerful and widely used machine learning algorithms which has been used to solve a range of engineering problems, notably in statistical signal processing, pattern recognition, image analysis, and digital communication systems [16,17]. In the latter application, SVM was used as a new method for channel equalization [18] and for combating the both multipath induced ISI and the co-channel interference [19]. In this paper, we introduce a SVM algorithm in 8-SPAM and DCO-OFDM VLC system to improve the system performance. Without any prior information or heuristic assumption, the SVM can be used to construct a classify model from a few training data set. Following training SVM is able to know about (i.e., learn) the properties of received signal and generate an improved decision hyperplane for more precise data detection. Moreover, through kernel function, the SVM becomes a nonlinear classifier, which is useful for higher level modulation schemes and for combating the errors caused by both the phase and amplitude noise. In order to test the bit-error rate (BER) performance of SVM-based one-dimensional and two-dimensional VLC systems. We have developed two experimental test-beds for full system evaluation. The results show that the SVM detection scheme can achieve improved performance when compared with the traditional DD method. We show that the BER performance deteriorate with increasing R_d. However, compared to the DD method, the SVM detection display superior BER performance. At the BER limit of 1.0×10^{-3} the SVM detection offer a maximum data of 8.1 Mbps over a transmission span of 1.6 m compared to 5.8 Mbps for the 8-SPAM DD based system. This is due to the enhanced decision boundary based on the specific distribution of received signal, obtained during the training process, which could lead to a more accurate classification.

The structure of this paper is as follows. The operation of each technique is detailed in Section 2. The experiment setup and result of the SVM-based detection for 8-SPAM are described in Section 3. The experiment setup and result of the SVM-based detection for DCO-OFDM are presented in Section 4. Finally, Section 5 concludes this paper.

2. Operation principle

2.1. Concept of SVM

A SVM is fundamentally a two-class classifier, which could generate a hyperplane to classify two segments of data. Based on the statistical theory, SVM aims to find an optimal (maximize) margin, which is defined by the smallest distance between the hyperplane and any point of the samples, as is depicted in Fig. 1. A subset of the data points which determine the location of the hyperplane are known as the support vectors. For the two-class linearly separable problem in an n-dimensional feature space, the hyperplane can be described by:

$$h(x) = W^{\boldsymbol{T}}X + b = 0 \tag{1}$$

where W is the normal vector and b is the distance from the hyperplane to the origin. The hyperplane $h(x)$ is learned using a training data set $\{x_i, y_i\}$, $i = 1, \ldots, l$, where $x_i \in \mathbf{R}^n$, and $y_i \in \{+1, -1\}$. Note that the hyperplane $h(\boldsymbol{x})$ can classify the training samples correctly, given the following conditions: if $y_i = +1$, $h(\boldsymbol{x}) \geq 1$; and if $y_i = -1$, $h(\boldsymbol{x}) \leq -1$. The points that make $h(x) = +1$, or -1 are known as the support vector. The perpendicular distance from any point x in the sample space to the hyperplane is given by:

$$r = \frac{\left|W^T X_n + b\right|}{\left\|W\right\|} = \frac{y_n\left(W^T X_n + b\right)}{\left\|W\right\|} \tag{2}$$

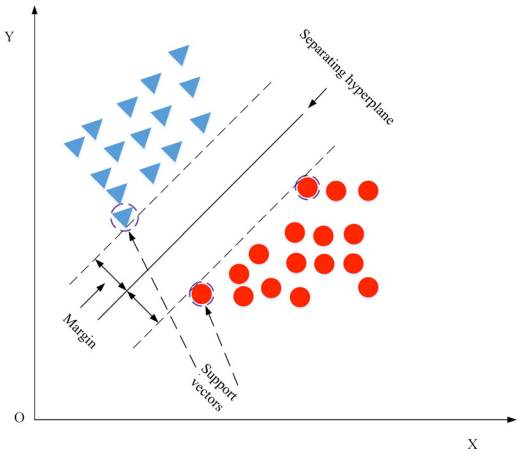

Fig. 1. SVM schematic diagram for linearly separable.

The goal of the SVM is to find a hyperplane in order to maximize the distance between the hyperplane and the training data points which are closest to the hyperplane. The problem, therefore, can be converted into the following equivalent convex quadratic problem:

$$\begin{aligned} &\min_{W,b} \frac{1}{2}\left\|W\right\|^2 \\ &s.t.\ y_i\left(W^{\boldsymbol{T}}x_i + b\right) \geq 1, \quad i = 1, 2, \ldots, N \end{aligned} \tag{3}$$

Using Lagrange multipliers (3) is written as:

$$\begin{aligned} &\max_{\alpha}\left\{\sum_{i=1}^{N}\alpha_i - \frac{1}{2}\sum_{i=1}^{N}\sum_{j=1}^{N}y_i \cdot y_j \cdot \alpha_i \cdot \alpha_j \cdot \left\langle x_i, x_j\right\rangle\right\} \\ &s.t.\sum_{i=1}^{N}\alpha_i y_i = 0, \\ &\alpha_i \geq 0, \quad i = 1, 2, \ldots, N \end{aligned} \tag{4}$$

Where the original problem is represented by $W = \sum_{i=1}^{N}\alpha_i y_i x_i$ and $0 = \sum_{i=1}^{N}\alpha_i y_i$. Therefore, having obtained Lagrange multipliers $\boldsymbol{\alpha}$, we can determine both $\boldsymbol{w}$ and b.

Usually, the data may overlap, thus making the exact separation of the training data challenging, which could lead to poor generalization. In this case, we introduce slack variables, which allow some of the training data to be misclassified in SVM. Adopting this approach results in a trade-off between the minimizing training errors and model complexity. Therefore, we have:

$$\begin{aligned} &\max_{\alpha}\left\{\sum_{i=1}^{N}\alpha_i - \frac{1}{2}\sum_{i=1}^{N}\sum_{j=1}^{N}y_i \cdot y_j \cdot \alpha_i \cdot \alpha_j \cdot \left\langle x_i, x_j\right\rangle\right\} \\ &s.t.\sum_{i=1}^{N}\alpha_i y_i = 0, \\ &0 \leq \alpha_i \leq C, \quad i = 1, 2, \ldots, N \end{aligned} \tag{5}$$

where C is the penalty factor, which corresponds to assigning higher penalties to the errors.

The SVM is very effective in solving linear classification problems. In practice, however, the data are usually linearly inseparable, see Fig. 1. Hence, the kernel trick [16] would be used to map linearly inseparable data from lower-dimensional feature space to higher-dimensional feature space. In the higher-dimension of the data, which in the original dimension is nonlinearly separable, is linearly separable, as depicted in Fig. 2. In this way, we can solve this linear classifying problem in higher-dimensions, which is equal to handling the nonlinear problem in the original dimension space. In this paper, we use the radial basis function (RBF) kernel which is commonly adopted in SVM classification. The RBF is defined as:

$$K\left(x_i, x_j\right) = \exp\left(-g \cdot \left\|x_i - x_j\right\|^2\right) \tag{6}$$

where $g > 0$ is the free parameter which determines the width of RBF.

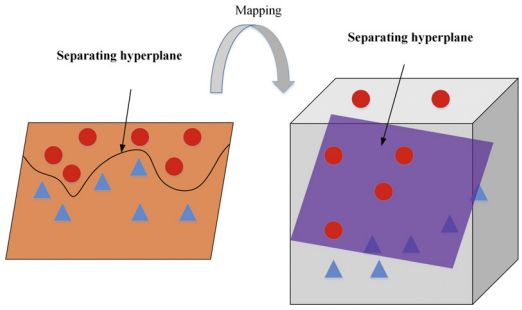

Fig. 2. using kernel function to realize linear classification for linearly inseparable data.

Following the introduction of the kernel function, (4) can be written as:

$$\begin{aligned} &\max_{\alpha}\left\{\sum_{i=1}^{N}\alpha_i-\frac{1}{2}\sum_{i=1}^{N}\sum_{j=1}^{N}y_i\cdot y_j\cdot\alpha_i\cdot\alpha_j\cdot k(x_i,x_j)\right\}\\ &s.t.\sum_{i=1}^{N}\alpha_i y_i=0,\\ &0\le\alpha_i\le C,\quad i=1,2,\ldots,N \end{aligned} \tag{7}$$

3. SVM for 8-SPAM detection

The basic concept of SPAM is to use multiple LEDs to realize digital to analog conversion in the optical domain [20,21]. Assuming I is the maximum light intensity for all independent LEDs, in order to generate an equally spaced PAM signal, the corresponding LED light intensities are set as: $I_1 = I/(2^{N-1})$, $I_2 = I/(2^{N-2})$, . . ., $I_k = I/(2^{N-k})$, . . . and $I_N = I$, where I_k is the intensity of kth LED, and N is the number of LEDs. Therefore, the equally spaced PAM signals could be generated by combining different optical intensity levels within the free space channel, which can also be considered as DAC of signal. Finally, the 2^N-level optical PAM signal can be detected at the Rx using only a single photo-detector (PD). A standard PAM demodulator can then be employed for de-mapping the received multi-amplitude signal back into the transmitted serial data stream. Therefore, by employing N-LEDs and a single PD, the SPAM scheme could achieve N time that of OOK employing a single LED and PD. Unlike OFDM and multi-band carrier-less amplitude and phase (CAP) modulation and multiple input multiple output (MIMO) scheme [22–24], which offers higher spectral efficiency, the SPAM scheme is a relatively simple not requiring complex data processing and DAC.

In this paper, three LEDs with different emitted light intensities are employed to realize the 8-SPAM scheme. Fig. 3(a) depicts the waveforms that drive the three LEDs, whereas Fig. 3(b) illustrates the corresponding combined 8-SPAM waveform and the signal mapping strategy. It is notable that the latter is the same as the traditional 8-PAM signal, therefore, an 8-PAM demodulator can be directly adopted for the proposed 8-SPAM scheme in order to recover the information.

As stated above, SVM is a two-class classifier as shown in Fig. 1 However, in many situations there is the requirement for classifying signals into multiple classes. Thus, a multi-class SVM classifier, which can be realized by combining multiple two-class SVMs, is needed. In this work, a 3-ary SVM is adopted as an 8-SPAM demodulator. With this approach, different amplitudes of 8-SPAM signals can be considered as eight different classes of the received data, which offer an improved decision boundary when using the SVM in comparison to the traditional DD based PAM. Note that in Fig. 4 each symbol bit is labeled as "+1" or "−1" by a binary SVM. For example, if a bit sequence of "110" is correctly detected by all three SVMs, then the least significant bit "0", the middle bit "1", and the most significant bit "1" are labeled as "−1" "−1" and "+1" by SVMs 1, 2 and 3, respectively. Since all permutations of the labels created by SVMs are unique, the combination of three SVMs could eventually perform as an 8-SPAM decoder.

Fig. 5(a) shows the system block diagram of the proposed SVM based 8-SPAM VLC system, which is composed of transmitter, channel, receiver and SVM signal detection module, whereas Fig. 5(b) illustrates the experimental setup. In the proposed prototype, a parallel data stream (i.e., SPAM) was first generated in Matlab, and then was applied to arbitrary waveform generator (AWG) (TTi TGA12104) to generate its electrical version for IM of three multi-chip white LED chips (Cree MC-E). The 3 dB modulation bandwidth of each LED chip is ∼2 MHz. At the Rx, combination of a condenser lens, and a PD (THORLABS PDA 10A-EC) was used to regenerate electric signal. A digital oscilloscope (Agilent DSO9104H) was used to capture the signal for further off-line signal processing in the Matlab domain. A 3-ary SVM model containing three SVMs was used for detecting of the captured signal. Since the SVM is able to acquire signal characteristics from the training data set for classification, no prior knowledge of the channel state information (CSI) is necessary. Finally, based on the output labels provided for the 3-ary SVM, mapping of the data to the corresponding symbols was carried out in the Matlab domain, as shown in Fig. 5(a). All the key system parameters are listed in Table 1.

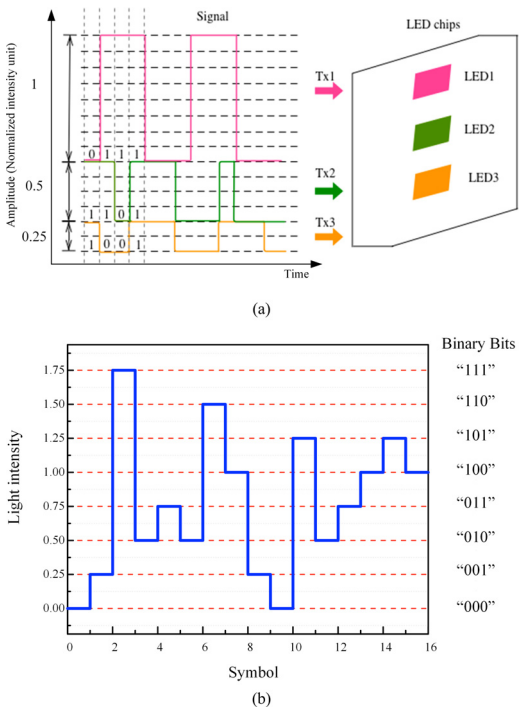

Fig. 3. 8-SPAM modulation scheme: (a) three waveforms that drive three LEDs, and (b) the corresponding combined waveforms and signal mapping strategy.

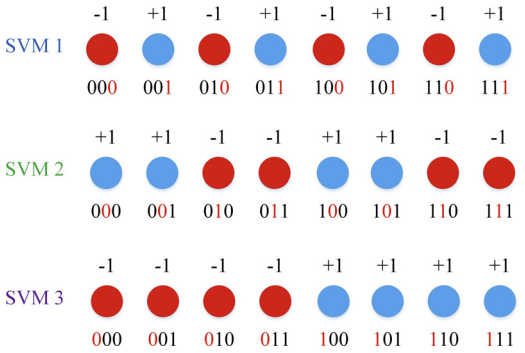

Fig. 4. Classification strategy based on SVM for 8-SPAM.

Table 1
Key parameters of experiment.

Parameter	Value
Transmission span	1.6 m
Data rate R_d	4.8–8.4 Mbps
Traning data set	6000 symbols
Half-angle of conser cup	35°
LED type	Cree MC-E
Transmit power	100mW
DC bias	0.45 A
Signal amplitude for each LED	500 mV_{pp}, 1 V_{pp}, 2 V_{pp}
LED 3 dB bandwidth	~2 MHz
PD bandwith	150 MHz
PD peak response	0.45 A/W (750 nm)
Condenser lens diameter	100 mm
Condenser lens focuals length	132 mm
SVM library	LibSVM [25]

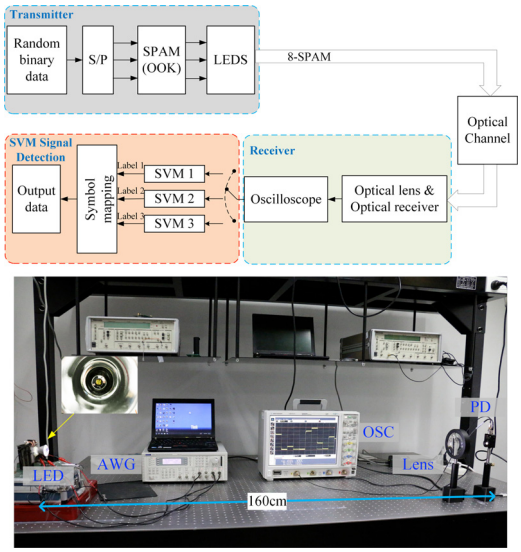

Fig. 5. SVM-based 8-SPAM VLC system: (a) block diagram and (b) experiment setup.

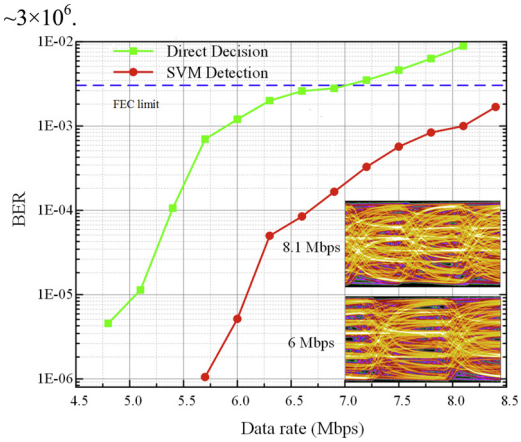

Fig. 6. BER as a function of transmission rates with SVMs detection and direct decision, insets present eye diagrams for SVM detection.

Note that, following completion of the training process, the received data was decoded using SVMs. The measured BER against the data rate performance for the SVM and DD based systems are shown in Fig. 6. For each data rate, the total number of recorded 8-SPAM symbols were $\sim 1 \times 10^6$. Therefore, the total number of raw binary bits was $\sim 3 \times 10^6$.

It can be inferred from Fig. 6 that the BER performance deteriorates with the increasing data rate. However, compared to the DD method, the SVM detection displays superior BER performance. For example, at a BER 1×10^{-5} the maximum data rates are ~5.1 Mbps and ~6.1 Mbps for DD and SVM detections, respectively. At the BER of 1.0×10^{-3} the SVM detection offers a maximum data of 8.1 Mbps over a transmission span of 1.6 m compared to the 5.8 Mbps for the DD detection based scheme. This is due to the enhanced decision boundary based on the specific distribution of the received signal, which was obtained during the training process, thus leading to a more accurate classification. Note that, the insets in Fig. 6 present two eye-diagrams for SVM detection with the data rates of 8.1 Mbps and 6 Mbps, and the BER of 1×10^{-3} and 5.16×10^{-6}, respectively.

Finally, Fig. 7 shows an example of the detection process based on using SVM to decode the 8-SPAM signal at R_d of 6 Mbps. The horizontal and vertical axis represents time and signal amplitude, respectively. In each subplot, the received signal corresponding labels of "+1" and "−1" are marked by the green symbols and the red symbols, respectively. As is depicted in Fig. 7, due to the limited LED bandwidth, the back-ground noise and the electrical noise, the constellations are fluctuating around the ideal constellation point. It is clear that SVM can obtain the characteristics from the training data and use them to adjust the decision boundary. By doing so, SVM can mitigate the impact of fluctuations, thus improving the BER performance of the link compared to the traditional DD VLC systems.

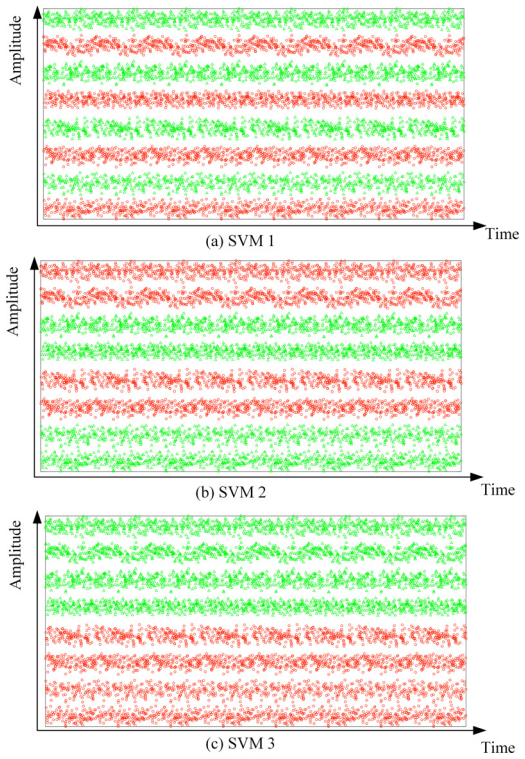

Fig. 7. 3-ary SVM detection examples for 8-SPAM with signal calssification by: (a) SVM1, (b) SVM2, and (c) SVM3.

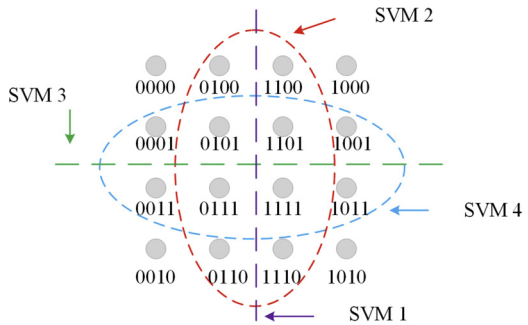

Fig. 8. Classification strategy for 16QAM with four SVMs.

4. SVM for DCO-OFDM detection

Next, we investigate the SVM method for detection of DCO-OFDM. Note that, in OFDM-VLC systems there are a number of issues including (i) reduced throughput due to the use of longer cyclic prefix [26]; (ii) performance degradation due to LED nonlinearity; and (iii) a high peak-to-average power ratio (PAPR), which result in severe distortion and clipping [2,26]. In order to alleviate this issue, we have proposed SVM to improve DCO-OFDM system performance.

M-QAM signal consists of *M* constellation points, each with in-phase (I) and a quadrature (Q) components. Hence, different constellation points of *M*-QAM can be seen as different class with two features for SVM. We design a multiclass classification SVM, in which only $\log_2 M$ SVMs are required for *M*-QAM. To illustrate the classification strategy based on SVM for DCO-OFDM, we have adopted 16-QAM with at least 4-SVM as an example as show in Fig. 8.

Fig. 9 shows the system block diagram of the proposed SVM based DCO-OFDM-16QAM VLC system. The DCO-OFDM signal generated in Matlab is applied to the AWG (Tektronix AFG3252) prior to IM of a red LED (Cree C503B). The red LED is used here because it has higher internal modulation bandwidth than the normal white LED. At the Rx, a combination of condenser lens, PD (THORLABS PDA 10A-EC), amplifier were used to regenerate the electric signal. A digital oscilloscope (Agilent MSOS404A) was used to capture the signal for further offline processing. Note that, to improve the system BER performance, we employed a low pass filter and a post-equalization in receiver side.

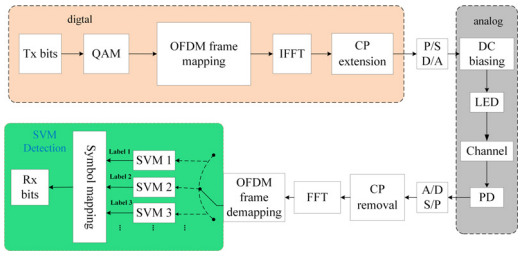

Fig. 9. Block diagram of experimental setup of the SVM detection based on DCO-OFDM.

Table 2
Key parameters of experiment.

Parameter	Value
Transmission span	0.3 m
Data rate R_d	232–328 Mbps
Traning data set	2^{12} symbols
PD bandwith	150 MHz
PD peak responsivity	0.45 A/W (750 nm)
Condenser lens diameter	100 mm
Condenser lens focuals length	132 mm
Kernel function	RBF
C and g	2.41, 0.32

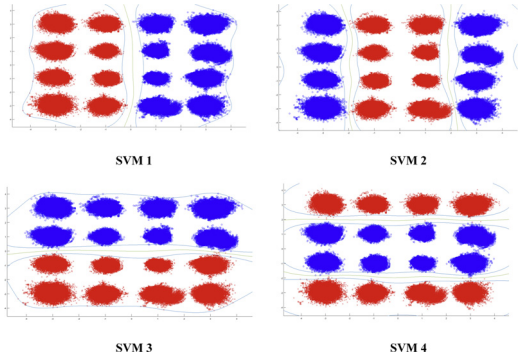

Fig. 10. The classification result of SVM detection for 16-QAM signal.

We used 2×10^{12} symbols as a training set. All the key system parameters are listed in Table 2. Note that, in SVM, both C and g are the key parameters that can affect SVM based detection performance. Here we have used cross-validation to obtain optimization of C and g in order to avoid the problem of overfitting or under-fitting, and achieve an improved performance.

Fig. 10 shows the constellation diagrams of SVM based detection applied to 16-QAM DCO-OFDM at a total R_d of 232 Mbps and EVM is 7.3. The constellation points in each subplot are divided into two categories, namely red and blue. The figure illustrates that constellation points are correctly classified by 4-SVM, however the outward divergence (or flattening) observed is mainly due to noise and nonlinear distortion. However, the classification curve constructed by SVM is smooth, thus illustrating that the proposed scheme offer improved classification of different types of constellation points.

The measured BER performance as a function of the R_d for both SVM and DD based systems is depicted in Fig. 11. At the lower R_d (i.e. <280 Mbps), SVM displays lower BER performance compared to DD. For example, at a R_d of 232 Mbps, the BER values are 5.67×10^{-6} and 1.17×10^{-6} for DD and SVM, respectively. However, as can be inferred from Fig. 11 the BER performance deteriorate with increasing R_d, (also see inset constellation diagram). For R_d > 280 Mbps both schemes display almost the same BER performance. This is because with R_d increasing the nonlinear and phase induced distortions are no longer the major factors in signal distortion.

5. Conclusion

In this paper, we presented an experimental VLC system using SPAM and DCO-OFDM modulation to realize data transmission for an indoor environment. The SVM scheme, which makes accurate decision in symbol detection, was employed to obtain the optimum decision boundary for decoding the SPAM signal. The experimental results indicated a maximum data rate of 8 Mbps at a BER of 1×10^{-3} can be archived using the SVM scheme over a communication range of 1.6 m. This is an increase of ~35% compared with the DD scheme. Additionally, we designed classification strategy based on SVM for DCO-

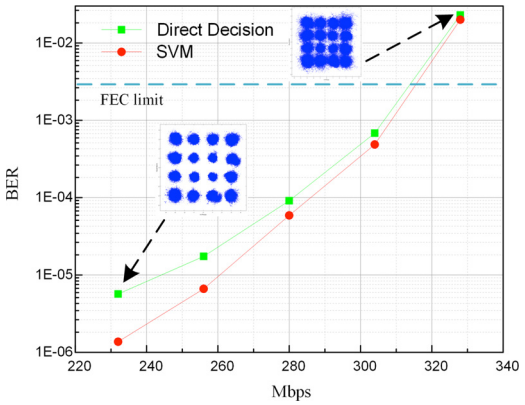

Fig. 11. BER as a function of transmission rates for both SVM and DD.

OFDM-16QAM. The experiment results show that BER performance is improved with the help of SVM when liner distortion is not a major factor in signal distortion.

As far as future work is concerned, other machine learning algorithms [27], such as K-nearest neighbor algorithm, K-means and artificial, are also potential algorithms to study in VLC system.

Acknowledgment

Portions of this work were presented at the conference CSNDSP in 2016, paper {paper number 1570252635}.

This work was supported by NSFC Project [grant numbers 61471052], Doctoral Scientific Fund of MOE of China [grant numbers 20120005110010] and the Royal Society Newton International Exchanges between U.K. and China [grant numbers NI140188], and by Science and Technology on Information Transmission and Dissemination in Communication Networks Laboratory [grant numbers ITD-U14005/KX142600012].

References

[1] S. Dimitrov, H. Haas, Principles of LED Light Communications: Towards Networked Li-Fi, Cambridge University Printing House, Cambridge CB2 8BS, United Kingdom, 2015.
[2] M. Uysal, C. Capsoni, Z. Ghassemlooy, A.C. Boucouvalas, E.G. Udvary (Eds.), Optical Wireless Communications – An Emerging Technology, Springer, Cham, Switzerland, 2016.
[3] Z. Ghassemlooy, W. Popoola, S. Rajbhandari, Optical Wireless Communications: System and Channel Modelling with Matlab®, CRC Press Taylor & Francis Group, Boca Raton, 2012.
[4] H. Elgala, R. Mesleh, H. Haas, Indoor optical wireless communication: potential and state-of-the-art, Commun. Mag. IEEE 49 (2011) 56–62.
[5] H. Li, X. Chen, B. Huang, D. Tang, H. Chen, High bandwidth visible light communications based on a post-equalization circuit, Photonics Technol. Lett. IEEE 26 (2014) 119–122.
[6] O. González, R. Pérez-Jiménez, S. Rodriguez, J. Rabadán, A. Ayala, OFDM over indoor wireless optical channel, in: Optoelectronics, IEE Proceedings, 2005, pp. 199–204.
[7] Z. Zhan, M. Zhang, D. Han, P. Luo, X. Tang, et al., 1.2 Gbps non-imaging MIMO-OFDM scheme based VLC over indoor lighting LED arrangements, in: Opto Electronics and Communications Conference (OECC), 2015, IEEE International Conference on.
[8] T. Fath, H. Haas, M.D. Renzo, R. Mesleh, Spatial modulation applied to optical wireless communications in indoor LOS environments, in: Global Telecommunications Conference (GLOBECOM 2011), 2011 IEEE, 2011, pp. 1–5.
[9] L. Song, P. Luo, M. Zhang, Z. Ghassemlooy, D. Han, H.L. Minh, Undersampled digital PAM subcarrier modulation for optical camera communications, Asia Communications and Photonics Conference 2015, Hong Kong, 2015, p. AM1E. 2.
[10] S.H. Yang, D.H. Kwon, S.J. Kim, S.K. Han, Overcoming bandwidth limitation of light – emitting diode in visible light communication using differential pulse amplitude modulation, Opt. Eng. 54 (2015) 126102.
[11] J. Li, Z. Huang, R. Zhang, F. Zeng, M. Jiang, Y. Ji, Superposed pulse amplitude modulation for visible light communication, Opt. Exp. 21 (2013) 31006–31011.
[12] C.M. Bishop, Pattern Recognition and Machine Learning, Springer, New York, 2006.
[13] S. Rajbhandari, Z. Ghassemlooy, M. Angelova, Effective denoising and adaptive equalization of indoor optical wireless channel with artificial light using the discrete wavelet transform and artificial neural network, J. Lightwave Technol. 27 (2009) 4493–4500.
[14] S. Rajbhandari, P.A. Haigh, Z. Ghassemlooy, W. Popoola, Wavelet-neural network VLC receiver in the presence of artificial light interference, IEEE Photonics Technol. Lett. 25 (2013) 1424–1427.
[15] P.A. Haigh, Z. Ghassemlooy, S. Rajbhandari, I. Papakonstantinou, W. Popoola, Visible light communications: 170 Mb/s using an artificial neural network equalizer in a low bandwidth white light configuration, J. Lightwave Technol. 32 (2014) 1807–1813.
[16] D. Wang, M. Zhang, Z. Li, Y. Cui, Nonlinear decision boundary created by a machine learning-based classifier to mitigate nonlinear phase noise, 2015, Optical Communication (ECOC) European Conference on IEEE, 2015, pp. 1–3.
[17] D. Wang, M. Zhang, Z. Cai, Y.Z. Cui, Z. Li, Combatting nonlinear phase noise in coherent optical systems with an optimized decision processor based on machine learning, Opt. Commun. 369 (2016) 199–208.
[18] D. Sebald, J. Bucklew, Support vector machine techniques for non linear equalization, IEEE Trans. Sig. Proc. 48 (2000) 3217–3266.
[19] J.P. Dubois, M. Abdul-Latif, Improved M-ary signal detection using support vector machine classifiers, Proc. World Acad. Sci. Eng. Technol. 7 (Aug) (2005) 264–268.
[20] J. Armstrong, Optical domain digital-to-analog converter for visible light communications using LED arrays [Invited], Photonics Res. 1 (2013) 92–95.

[21] J. Yew, S.D. Dissanayake, J. Armstrong, Performance of an experimental optical DAC used in a visible light communication system, in Globecom Workshops (GC Wkshps), 2013 IEEE, 2013, pp. 1110–1115.
[22] S.D. Dissanayake, J. Armstrong, Comparison of ACO-OFDM, DCO-OFDM and ADO-OFDM in IM/DD systems, J. Light. Technol. 31 (7) (2013) 1063–1072.
[23] K. Werfli, P.A. Haigh, Z. Ghassemlooy, P. Chvojka, S. Zvanovec, S. Rajbhandari, Shihe Long, Multi-band carrier-less amplitude and phase modulation with decision feedback equalization for bandlimited VLC systems, in: 2015 4th International Workshop on Optical Wireless Communications (IWOW), 2015, pp. 6–10.
[24] C.W. Hsu, C.W. Chow, I.C. Lu, Y.L. Liu, C.H. Yeh, Y. Liu, High speed imaging 3×3 MIMO phosphor white-light LED based visible light communication system, IEEE Photonics J. 8 (Dec (6)) (2016) 1–6.
[25] C.-C. Chang, C.-J. Lin, LIBSVM: a library for support vector machines, ACM Trans. Intell. Syst. Technol. 2 (2011) 27.
[26] T. Tao Jiang, Y. Yiyan Wu, An overview: peak-to-average power ratio reduction techniques for OFDM signals, IEEE Trans. Broadcast. 54 (Jun (2)) (2008) 257–268.
[27] D. Wang, M. Zhang, M. Fu, Nonlinearity mitigation using a machine learning detector based on k-nearest neighbors, IEEE Photonics Technol. Lett. 28 (19) (2016) 2102–2105.